NASA TN D-1636

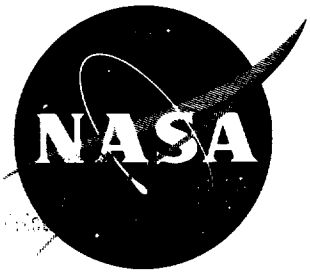

TECHNICAL NOTE

D-1636

A THEORETICAL STUDY OF THE MOTION OF AN IDEALIZED PLASMA RING THROUGH VARIOUS TRAVELING-MAGNETIC-WAVE PLASMA ACCELERATORS

By Clarence W. Matthews

Langley Research Center
Langley Station, Hampton, Va.

NATIONAL AERONAUTICS AND SPACE ADMINISTRATION

WASHINGTON May 1963

NATIONAL AERONAUTICS AND SPACE ADMINISTRATION

TECHNICAL NOTE D-1636

A THEORETICAL STUDY OF THE MOTION OF AN IDEALIZED PLASMA RING THROUGH VARIOUS TRAVELING-MAGNETIC-WAVE PLASMA ACCELERATORS

By Clarence W. Matthews

SUMMARY

The results of several computations of the motion of idealized plasma rings under the influence of several different traveling-magnetic-wave accelerators are presented and analyzed to show some of the theoretical phenomena that can occur in such accelerators. The results indicated that only a narrow range of magnetic-field and plasma-ring characteristics existed in which the plasma ring was confined within the accelerator. Slippage of the ring with respect to the field was observed in all the computations made. Comparison with available experimental data showed almost an order-of-magnitude reduction in velocity resulted from experimental effects.

INTRODUCTION

Several reasons for proposing traveling-magnetic-wave systems for the acceleration of neutral plasma are based on the considerations that the plasma generally follows or "sticks" to the magnetic-field lines and that the magnetic field will more or less contain the plasma. (See refs. 1 and 2, for example.) Experimental data presented in reference 3 indicate that the plasmoid velocity was close to the magnetic-wave velocity; however, the problem of synchronization of the plasma with the magnetic field was not studied. In another experiment, reference 4, neither containment of the plasma nor acceleration to the magnetic-field velocity seemed to be attained. These partial failures seemed most likely a result of the fact that the gas was only partially ionized so that interferences between the neutral and ionized particles occurred and prevented ideal operation of the system.

Since information on both synchronization and containment was rather difficult to obtain experimentally, it was believed that several computations of the motion of an ideal plasma ring through various traveling-magnetic-wave plasma accelerators by use of the methods presented in reference 5 might give some information on the nature of the conditions required for the synchronization of plasma-ring motion with magnetic-field motion and for the containment of the ring within the confines of the accelerator.

It is the purpose of this paper to present the results of several such calculations showing some of the problems involved with the synchronization of the plasma motion to the magnetic-wave motion and with the containment of the plasma itself and indicating conditions under which the ideal traveling-wave accelerator can be expected to perform successfully.

SYMBOLS

The rationalized mksq system of units is used herein.

B	nondimensional drive intensity factor, $\mu_o eI/4\pi m_e \omega R$
e	charge on a singly charged ion
I	maximum value of alternating drive current
m_e	mass of an electron
m_i	mass of a single ion
n	number of ions or electrons in plasma ring
R	radius of drive coil
r	radius of plasma ring
t	time
x	axial location of plasma ring
β	ratio of m_i/m_e
$\zeta = n \times 10^{-15}/R$	
μ_o	permeability of free space, $4\pi \times 10^{-7}$ h/meter
φ	phase angle of drive current
$\dot{\theta}_i$	time rate of change of the angular position of the ions
$\dot{\theta}_e$	time rate of change of the angular position of the electrons
ω	angular frequency of drive current

Subscript:

o value of parameter at starting position of accelerator

Dots over symbols represent differentiation with respect to time.

THEORY

The theory by which the motion of an ideal plasma ring in a traveling-magnetic-wave accelerator was calculated involved adaptation of the total differential equation of motion of charged particles in a magnetic field to the problem of the motion of an ideal neutral plasma ring in an axial magnetic field. The basic theory of this adaptation is presented in detail in reference 5 and will be but briefly discussed herein. The development involves several simplifications of the physical nature of a plasma ring. The basic assumptions are: no collision effects, single ionizations of all the atoms or molecules in the ring, equal numbers of ions and electrons, all particles concentrated on the circle through the centers of gravity of the cross sections of the ring, and that the plasma-ring resistance is small compared with the inductive reactance of the ring. These assumptions are required to permit the plasma-ring motion to be expressed by a total differential equation. The reason for using such an equation rather than an equation such as the Boltzman equation (ref. 6, p. 18) is that total differential equations are more readily integrated by electronic data processing systems.

The actual equations were developed by writing the Lagrangian equations of the motion of a charged mass in a magnetic field for both the ions and the electrons. These were then combined with the constraint that the axial and radial positions and motions of both the ions and electrons must remain the same during the entire motion. These expressions were then substituted into the Lagrangian equations to obtain the differential equations of motion given in reference 5.

COMPUTATION OF ACCELERATORS

The first accelerator (I) computed consisted of 14 turns of equal radius R located as shown in figure 1(a). The actual coil locations computed are given in table I. The first two coils are compensation coils and are not a part of the accelerator but are used to cancel the field created by coils 4 and 5 at the time of starting. These were added because of the irregular paths found to occur when the ring is started in the presence of a magnetic field (ref. 5). The accelerator actually consists of coils 3 to 14. The coils are driven by a three-phase system, that is, coils 3, 6, 9, and 12 are connected to phase 1, coils 4, 7, 10, and 13 to phase 2, and coils 5, 8, 11, and 14 to phase 3, and all turns are wound in the same direction. The coils are spaced such that if a charged particle starts under coil 3 at a velocity of $0.044\omega R$ (where ω is the angular frequency of the drive system) and accelerates with a linear-velocity increase to a velocity of $0.44\omega R$ under coil 14 then that particle will be approximately synchronized with the magnetic-field motion. Thus, accelerator I should theoretically increase the

input velocity by about a ratio of 10 provided the plasma synchronizes with the field and does not slip a quarter wave or more.

The second and third systems (II and III) computed had the same coil spacing with the exception that the starting-field compensation coils were omitted (fig. 1(b)) and an additional set of coils was added with the same axial spacing and of 1/2 the radius of those in accelerator I. The difference between system II and system III is in the direction of the flow of the currents in the inner coil. In system II, the current in each of the inner coils flows in the same direction as in its corresponding outer coil whereas in system III the current flow in each of the inner coils is in the direction opposite to that of the outer coil. The effect of these current directions is to produce a field predominately normal to the accelerator axis in the center of the region between the two coils in accelerator II and correspondingly a predominately parallel field in system III.

Computations were also made on a fourth system (IV) with coil locations and conditions corresponding to those presented in reference 4. The locations of these coils and current phase angles are shown in table I. The alternating-current-excited drive coils were equally spaced and each coil lagged its predecessor by 90°, making a four-phase system of the accelerator.

An IBM 7090 electronic data processing system was used to integrate the equations of motion. It was programed to print the following values: x/R, $\dot{x}/\omega R$, r/R, $\dot{r}/\omega R$, $r\dot{\theta}_e/\omega R$, $r\dot{\theta}_i/\omega R$, and ωt where x and r are the axial and radial coordinates of the ring, $\dot{\theta}_e$ and $\dot{\theta}_i$ are the azimuthal velocities of the electrons and ions, respectively, and t is time.

Typical paths, plots of r/R against x/R, of the plasma ring in the various accelerators and under various acceleration conditions are shown in figures 2 to 5. In these figures the symbols with zero subscripts indicate the initial value of the quantity at the start of the motion. A plot of ζ against B is given in figure 6, which shows the region of successful operation of accelerators I and IV. Plots of x/R against ωt are presented in figure 7 to show both synchronous and asynchronous ring motions.

ANALYSIS OF RESULTS

Plasma-Ring Paths

Several of the computed paths that an ideal plasma ring can take as it is accelerated by a traveling-magnetic-wave accelerator are shown in figures 2 to 5. Analysis of these paths shows that successful operation of the system occurs only for a rather narrow range of values of B for a given plasma ring. It was observed in the case of accelerator I, the 14-coil accelerator, that the paths of the successful conditions were quite similar over a large variation in ζ, whereas the paths of the unsuccessful, i.e., escape conditions where the ring goes through the coil, as in figure 3(a) or becomes stalled as in figures 2(a) and 2(c), did not show such similarities. Apparently once the ring attains a condition wherein it can no longer follow the magnetic-field wave, its path can change very much with only small changes in the acceleration conditions.

Some of the effects of generally normal and generally parallel magnetic fields on the acceleration of plasma rings can be seen by comparing the results presented in figures 3 and 4. It is seen that the normal field performed a smooth, successful acceleration whereas no such acceleration was made by the parallel field. One apparently successful acceleration did occur; however, the ring went inside the inner coils and hence escaped from the desired acceleration region.

The four-phase system, accelerator IV, showed successful paths similar to those observed in the other accelerators (fig. 5). In fact these paths are smoother in that they do not close to as small a radius as seen in the paths shown in figure 2(b).

Successful Operating Condition

A plot of $\log \zeta$ against $\log B$ is shown in figure 6, in which each point indicates the values of ζ and B for a particular acceleration condition with accelerator I or IV as the driver. The circles indicate successful operation and the squares indicate failure by either escape or stall. Within the scope of the computations made, it would seem from examination of figure 6 that any region of successful operation is restricted to a narrow range of values of ζ and B, such that $\log \zeta$ seems to be a linear function of $\log B$. The slope of the $\log \zeta, \log B$ curve is seen to be about 2 when $\log \zeta$ is greater than 1, indicating that under these conditions the values of ζ for successful operation vary as the square of B. This may be restated by saying that the ratio $I/\omega R$ must be increased with the square root of the number of particles in the ring, provided the plasma ring has greater than 10^{15} particles per meter radius, i.e., $\zeta = 1$. It is also observed that if the plasma ring has less than 10^{15} particles per meter radius then no or very little reduction can be made in the value of B or $I/\omega R$ if successful operation is to be achieved. These phenomena indicate that a certain minimum condition must exist in a traveling-wave accelerator and also that careful matching of the factor $I/\omega R$ and the mass of the ring must be made if confined acceleration is to occur.

The cross-hatched area shows the region of experimental operation indicated in reference 4. Several computations showed that this region is one of successful operation. However, the calculated output velocity was appreciably higher, $1.226\omega R$ as opposed to the $0.136\omega R$ reported. In fact, the value $1.226\omega R$ is almost twice the velocity of the magnetic wave, $0.6342\omega R$, thus indicating that the ring was sliding forward on the magnetic field and was not locked to it. The wide discrepancy between the theoretical and experimental velocities is believed to be due to the low percentage of ionization and the interactions between the ions and the neutrals. That is, the ions were slowed down by being caused to drag the neutrals along by collision effects.

Plasma-Ring and Magnetic-Field Motion

Several indications of the relations existing between the motion of the plasma ring and that of the magnetic field are shown in figures 7 to 10. These figures present plots of the axial location x/R and the axial velocity $x/\omega R$

of several plasma rings and their corresponding magnetic fields as functions of ωt. The plots are shown for accelerators I and IV. The conditions for each computation are shown in the figures.

It is seen from figure 7 that for the computation $B = 14$ and $\zeta = 1$, the ring locked onto the second magnetic wave and traversed the accelerator successfully (see also fig. 2(b)). The other rings, accelerated at $B = 10$, 17.6, and 20, were in synchronization with the second wave for values of ωt between 15 and 25 but could not hold, and so slipped back over the magnetic wave and hence out of synchronization. Also, once the break was made these rings could not relock onto the magnetic field. These figures show that plasma rings even though infinitely conductive do not necessarily stick to the magnetic-field lines. The observation that the plasma rings do not seem to be frozen to the magnetic-field lines is explained at least in part in reference 6 (sec. 3-2) with the argument that the plasma-ring motions and rates of change of the external magnetic fields are too great for the plasma rings to be frozen to the magnetic-field lines.

This phenomenon is also seen in the four-phase system of reference 4 (see fig. 8). Here the successfully accelerated ring jumps ahead of the magnetic wave. This increase of ring velocity over magnetic-field velocity shows that the ring can slide ahead on the magnetic wave and so obtain an excess velocity. It is also seen that the two rings containing the greater number of particles, i.e., $\zeta = 0.65$ and $\zeta = 2.025$ do not accelerate sufficiently even to synchronize, let alone slide down the magnetic wave. As a result they become lost to the magnetic field. As before, if synchronization does not occur within one or two passes of the magnetic field, it does not seem to have much chance of occurring.

More details of the axial-velocity changes can be seen in figures 9 and 10. These figures show plots of the reduced axial velocity $\dot{x}/\omega R$ as functions of the reduced time ωt for plasma rings traveling through the 14-coil, three-phase accelerator I (fig. 9), and through the 4-coil, two-phase system IV, figure 10. It is seen that the motion of the ring which successfully traverses the three-phase system, figure 9, is quite irregular and obviously does not stick to the magnetic field but tends to oscillate back and forth on the wave. Oscillations in the axial direction are even more pronounced for those rings which did not traverse the accelerator, i.e., $B = 10$ and 17.6.

Fewer oscillations are seen in the ring motion of the 4-coil, four-phase system as shown in figure 10. These rings also do not lock onto the magnetic wave but are accelerated to a much higher velocity by a single-coil type of action. Then they are slowed down by the coils ahead or by running ahead on the magnetic wave to a point where the gradient is in the opposite direction.

Strong azimuthal oscillations were also observed in the three-phase case, as is seen in figure 11, which shows plots of $r\dot{\theta}_e/\omega R$ as functions of ωt. These azimuthal oscillations could be similar to those reported in reference 3 in which such oscillations were recorded by a magnetic-coil pickup placed slightly ahead of the accelerator.

Comparison With Single-Coil Accelerators

It is interesting to compare the theoretical velocities obtained in the successfully operating traveling-wave accelerator with those obtained in a single-coil accelerator operating with the same drive-coil current. If such a comparison is made between the data of reference 5 and the final velocities of the traveling-wave systems as presented in figure 6 several interesting points may be noted. In the case of the 14-coil system or accelerator I the value of B for successful operation using an H^+ plasma ring with 10^{15} ions per meter, or $\zeta = 1$, is about 14 or a value of $I/\omega R$ of about 0.00078. If these values are looked up in figure 7 of reference 4 it will be found that the axial velocity is about $0.69\omega R$ as compared to the value of $0.60\omega R$ for the equivalent traveling-wave system. The 24-coil normal-field system, accelerator II, has an output velocity of $0.7\omega R$ for $B = 5.25$ as compared with the output velocity, $0.25\omega R$, of the single-coil system. In the accelerator given in reference 5, the 4-coil, four-phase system, the magnetic-wave velocity is $0.63416\omega R$ whereas the computed plasma-ring velocity is about $1.2\omega R$ and the single-coil plasma-ring velocity is, from reference 5, about 0.9 to $1.0\omega R$.

The interesting point to note is that the single-coil system, theoretically at least, can produce velocities that are comparable to the velocities attained in the more complex traveling-wave system.

Sequence-Fired and Continuously Operating Systems

Three modes of operation can be used on the traveling-wave system. One is the sequence-fired mode in which each coil is energized from its own condenser and switch. This system is more adaptable to a pulse-type system using large plasmoids. The second system is a lumped-parameter transmission line (ref. 3) and is very similar in operation to the sequence-fired system. The third system is a continuously operated accelerator in which every coil is energized during the entire acceleration process, as represented by the experiments of reference 4. This system is believed to be more adaptable to a continuous-flow process which uses much smaller plasma rings. The theory used in this study is adapted to the continuous system, but possibly a few conclusions may be carried over to the other system.

It is believed that a minimum value of $I/\omega R$ is required to accelerate a plasmoid in phase with the magnetic wave of the accelerator. Certainly if the field is too weak or the value of $I/\omega R$ too small then a situation similar to the theoretical situation under consideration will be involved wherein the magnetic wave will get ahead of the plasma and so the ring can no longer lock onto the magnetic wave. The result is of course no acceleration. In case the field strength is too high, that is, if $I/\omega R$ is too large, then it is possible for the plasma ring to get out of or ahead of the magnetic field and then no longer be contained by it and so escape to the wall by both centrifugal and pressure forces. Escape to the wall can cause several undesirable effects such as deionization, lack of synchronization, loss of velocity, and excessive wall heating.

It would thus appear from this analysis that careful matching of the magnetic-field intensity to the plasma-ring mass is required for successful operation regardless of the mode of operation used for the accelerator.

The argument that a minimum value of $I/\omega R$ is required for a system operated with a shock front is also believed to hold. However, the design values of $I/\omega R$ and ζ are probably quite different as ζ varies appreciably through the entire process. Also much of the ionized gas does not contribute to the plasma currents because of shallow field penetration. These factors may severely influence accelerator design, especially coil location.

CONCLUDING REMARKS

Computations made on the motion of idealized plasma rings in various traveling-magnetic-wave accelerators have shown several interesting features about such motions. First, in the accelerators studied, a combination of parameters involving magnetic-field strength, the number and mass of the particles in the ring could be found for which the ring traversed the accelerator successfully; however, this combination occurred over only a narrow range of values, thus restricting regions of successful operation.

Second, the plasma rings did not lock onto the magnetic fields but tended to oscillate over them.

Third, once the ring lost any semblance of synchronization with the magnetic field, sychronization was never regained, at least within the time range covered by the computation. Also, if the ring did not accelerate with the second or third wave, it did not accelerate with any of the following waves.

Fourth, the velocities attained in a 12-coil, three-phase system were of the order of the velocity of the magnetic wave, whereas those obtained in a 4-coil, four-phase system were above the synchronous velocity and of the order of the velocities obtained if one of the coils had been used as a single-coil accelerator.

Fifth, the theoretical velocities of the traveling-wave system computed and those obtained in a single-coil system are of the same order of magnitude.

Sixth, comparison of the theoretical velocities of a 4-coil, four-phase system with corresponding experimental velocities showed that the experimentally attained velocities were about an order of magnitude lower than the indicated theoretical velocities.

Langley Research Center,
National Aeronautics and Space Administration,
Langley Station, Hampton, Va., January 30, 1963.

REFERENCES

1. Clauser, Milton U.: The Magnetic Induction Plasma Engine. STL/TR-60-0000-00263, Space Tech. Labs., Inc., Aug. 19, 1960.

2. Meyer, Rudolf X.: Magnetic Plasma Propulsion by Means of a Traveling Sinusoidal Field. STL/TR-60-0000-09114, Space Tech. Labs., Inc., Apr. 30, 1960.

3. Marshall, John: Acceleration of Plasma Into Vacuum. Proc. Second United Nations Int. Conf. on Peaceful Uses of Atomic Energy (Geneva), vol. 31 - Theoretical and Experimental Aspects of Controlled Nuclear Fusion, 1958, pp. 341-347.

4. Jones, Robert E., and Palmer, Raymond W.: Traveling Wave Plasma Engine Program at NASA Lewis Research Center. Third Symposium on the Engineering Aspects of Magnetohydrodynamics, Univ. of Rochester, Mar. 28-29, 1962.

5. Matthews, Clarence W.: A Theoretical Study of the Motion of an Idealized Plasma Ring Under the Influence of Various Coaxial Magnetic Fields. NASA TR R-121, 1961.

6. Spitzer, Lyman, Jr.: Physics of Fully Ionized Gases. Interscience Publ., Inc. (New York), 1956.

TABLE I.- COIL LOCATIONS FOR ACCELERATORS I, II, AND III

x/R	$\frac{R_{outer}}{R}$	$\frac{R_{inner}}{R}$ (used on accelerators II and III)	Phase angle, φ
*-0.3979	1.0000	0.5000	$-4\pi/3$
*-.1514			$-2\pi/3$
0			0
.1514			$2\pi/3$
.3979			$4\pi/3$
.7383			0
1.1725			$2\pi/3$
1.7017			$4\pi/3$
2.3248			0
3.0421			$2\pi/3$
3.8537			$4\pi/3$
4.7595			0
5.7596			$2\pi/3$
6.8540			$4\pi/3$

*Coils not used on accelerators II and III.

COIL LOCATIONS FOR ACCELERATOR IV

Alternating-current-energized drive coils		
x/R	R	φ
0	1	0
1	1	$\pi/2$
2	1	π
3	1	$3\pi/2$

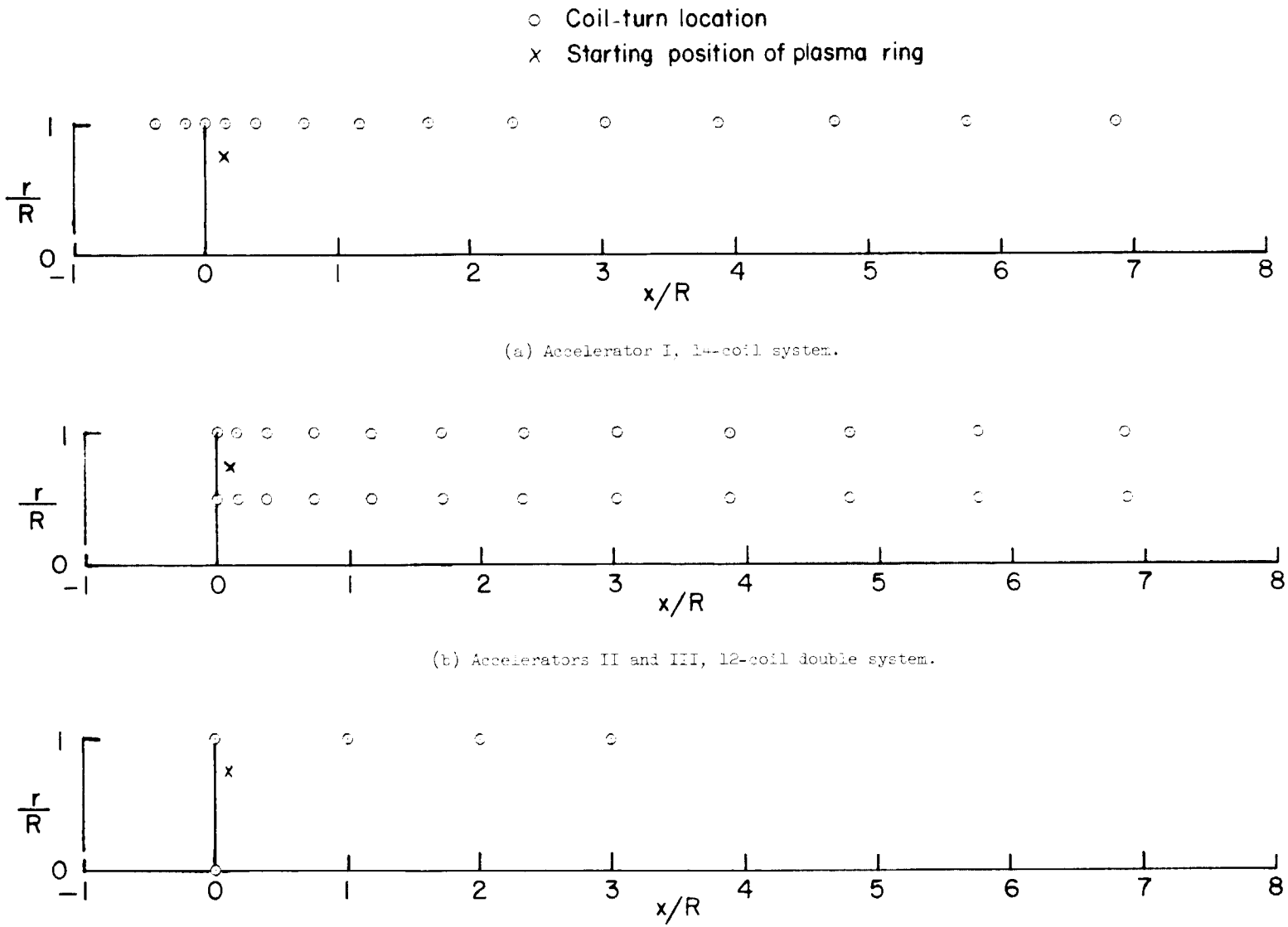

(a) Accelerator I, 14-coil system.

(b) Accelerators II and III, 12-coil double system.

(c) Accelerator IV, 4-coil, two-phase system.

Figure 1.- Sketch of coil-turn location and plasma-ring starting positions.

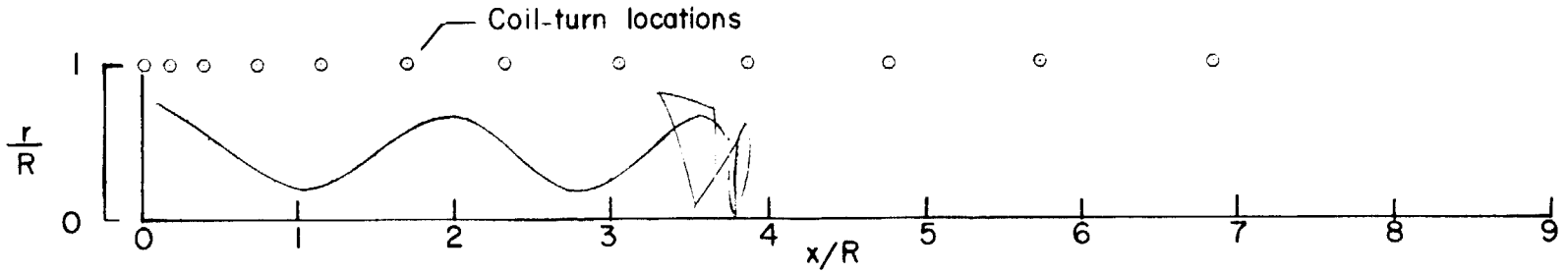

(a) B = 10 or $I/\omega R = 0.00568$; $\dot{x}_{final} = 0.0069\omega R$.

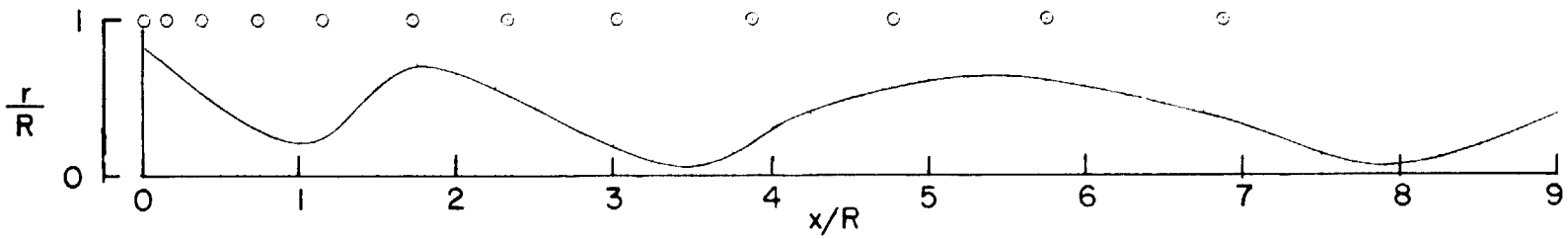

(b) B = 14 or $I/\omega R = 0.00796$; $\dot{x}_{final} = 0.6079\omega R$.

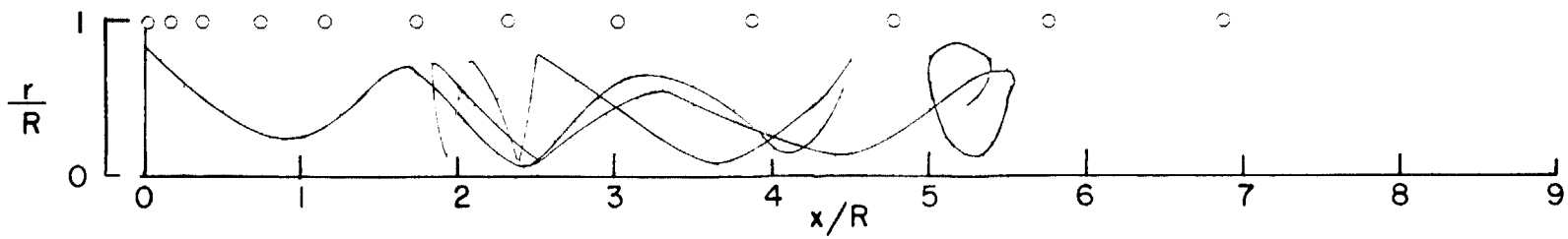

(c) B = 17.6 or $I/\omega R = 0.01000$; $\dot{x}_{final} = -0.1264\omega R$.

Figure 2.- Paths of a hydrogen plasma ring in the field of accelerator I, a 14-coil, three-phase traveling-magnetic-wave system. $n/R = 10^{15}$ or $\zeta = 1$; $\beta = 1,845$; starting conditions: $\dot{x}_o = 0.0447$, $\dot{r}_o = \dot{\epsilon}_o = 0$, $x_o/R = 0.1$, $r_o/R = 0.75$, $t = 0$.

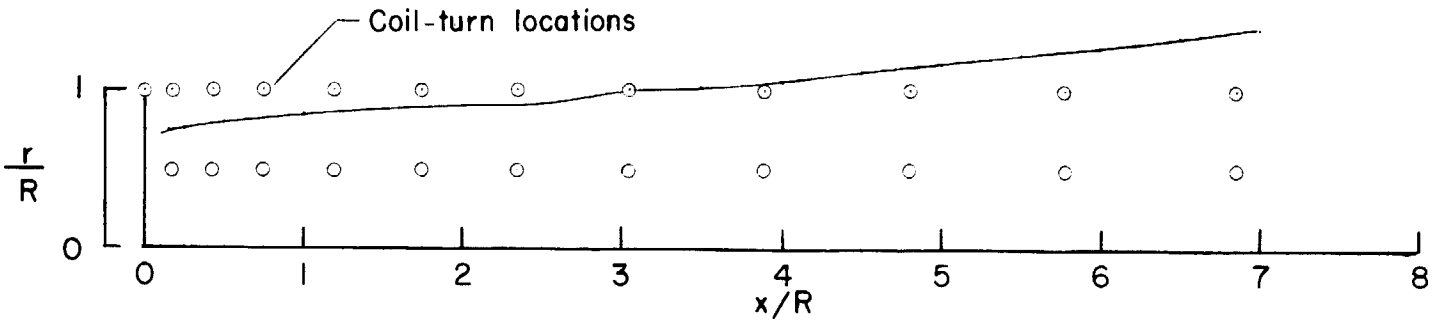

(a) B = 4.25 or $I/\omega R = 0.002416$; $\dot{x}_{final} = 0.4883\omega R$.

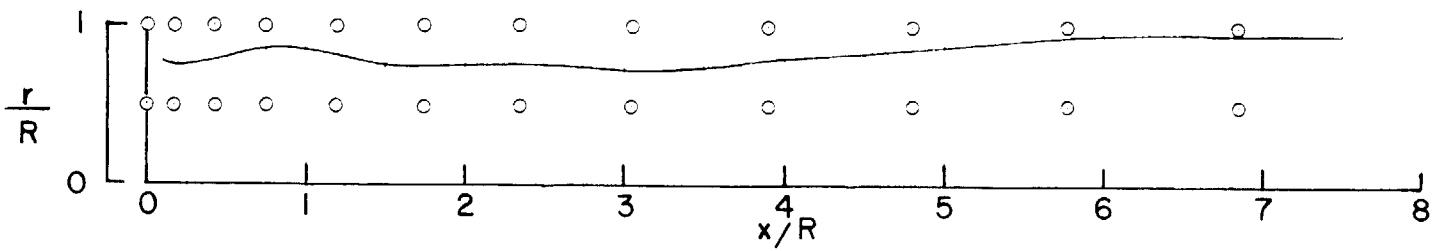

(b) B = 5.0 or $I/\omega R = 0.002842$; $\dot{x}_{final} = 0.5219\omega R$.

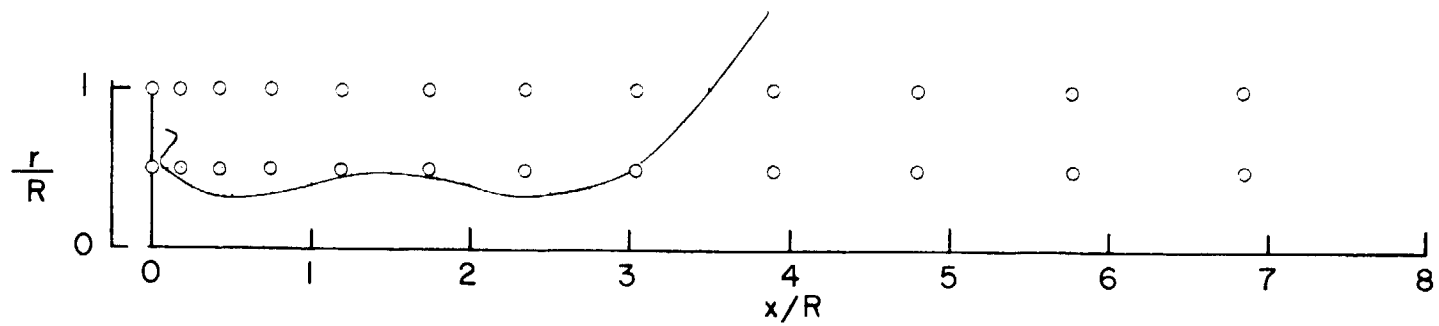

(c) B = 5.76 or $I/\omega R = 0.00327$; $\dot{x}_{final} = 0.07799\omega R$.

Figure 3.- Paths of a hydrogen plasma ring in the field of accelerator II, a 24-coil normal-field traveling-wave system. $n/R = 10^{15}$ or $\zeta = 1$; $\beta = 1.845$; starting conditions: $\dot{x}_o = 0.0447$, $r_o = \theta_o = 0$, $x_o/R = 0.1$, $r_o/R = 0.75$, $t = 0$.

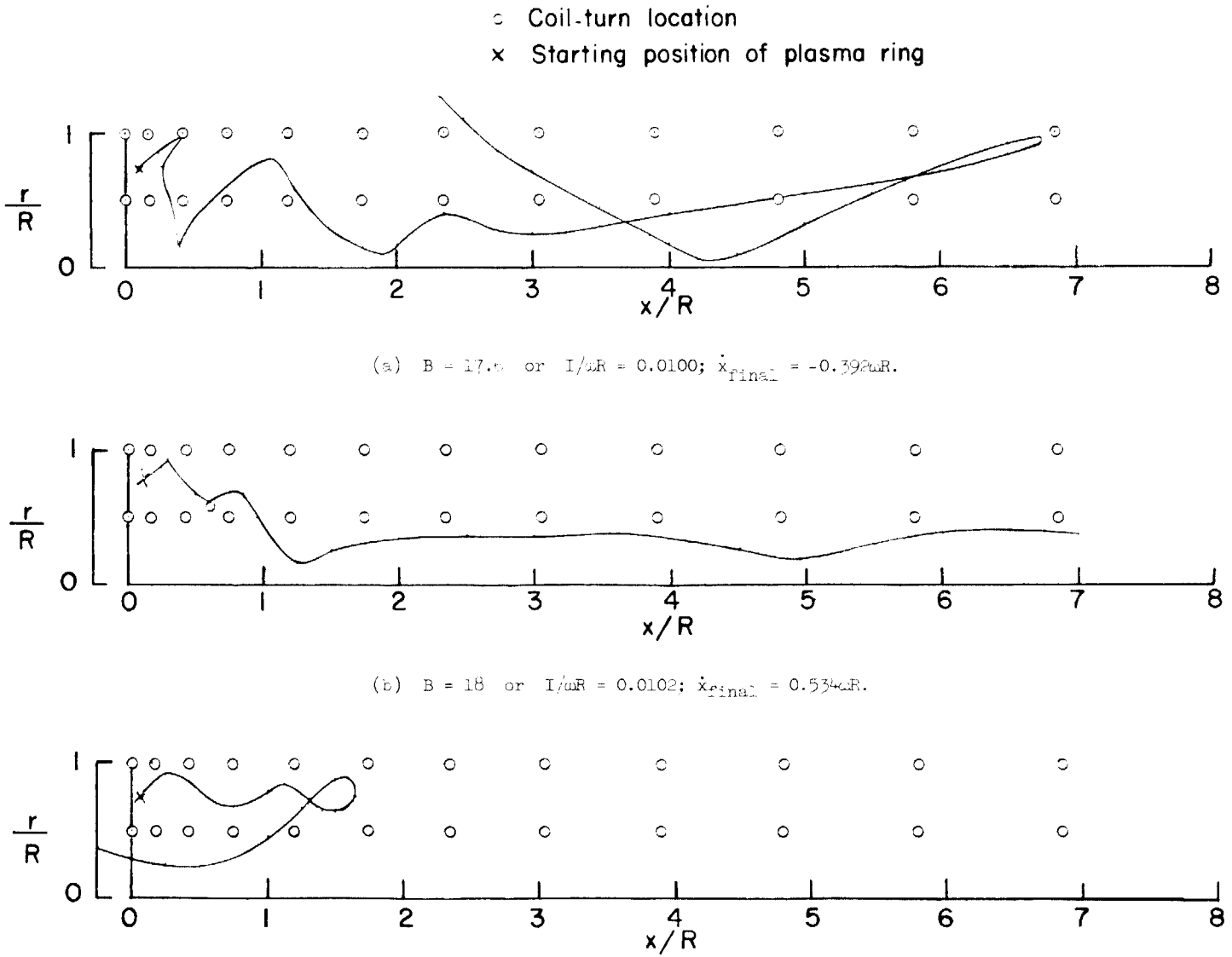

(a) B = 17.6 or $I/\omega R = 0.0100$; $\dot{x}_{final} = -0.392\omega R$.

(b) B = 18 or $I/\omega R = 0.0102$; $\dot{x}_{final} = 0.534\omega R$.

(c) B = 18.5 or $I/\omega R = 0.0105$; $\dot{x}_{final} = -0.335\omega R$.

Figure 4.- Paths of a hydrogen plasma ring in the field of accelerator III, a 24-coil parallel-field traveling-wave system. $n/R = 10^{15}$ or $\zeta = 1$; $\beta = 1.3 \times 5$; starting conditions: $\dot{x}_0 = 0.0447$, $r_0 = \theta_0 = 0$, $\dot{x}_0/R = 0.1$, $r_0/R = 0.75$, $t = 0$.

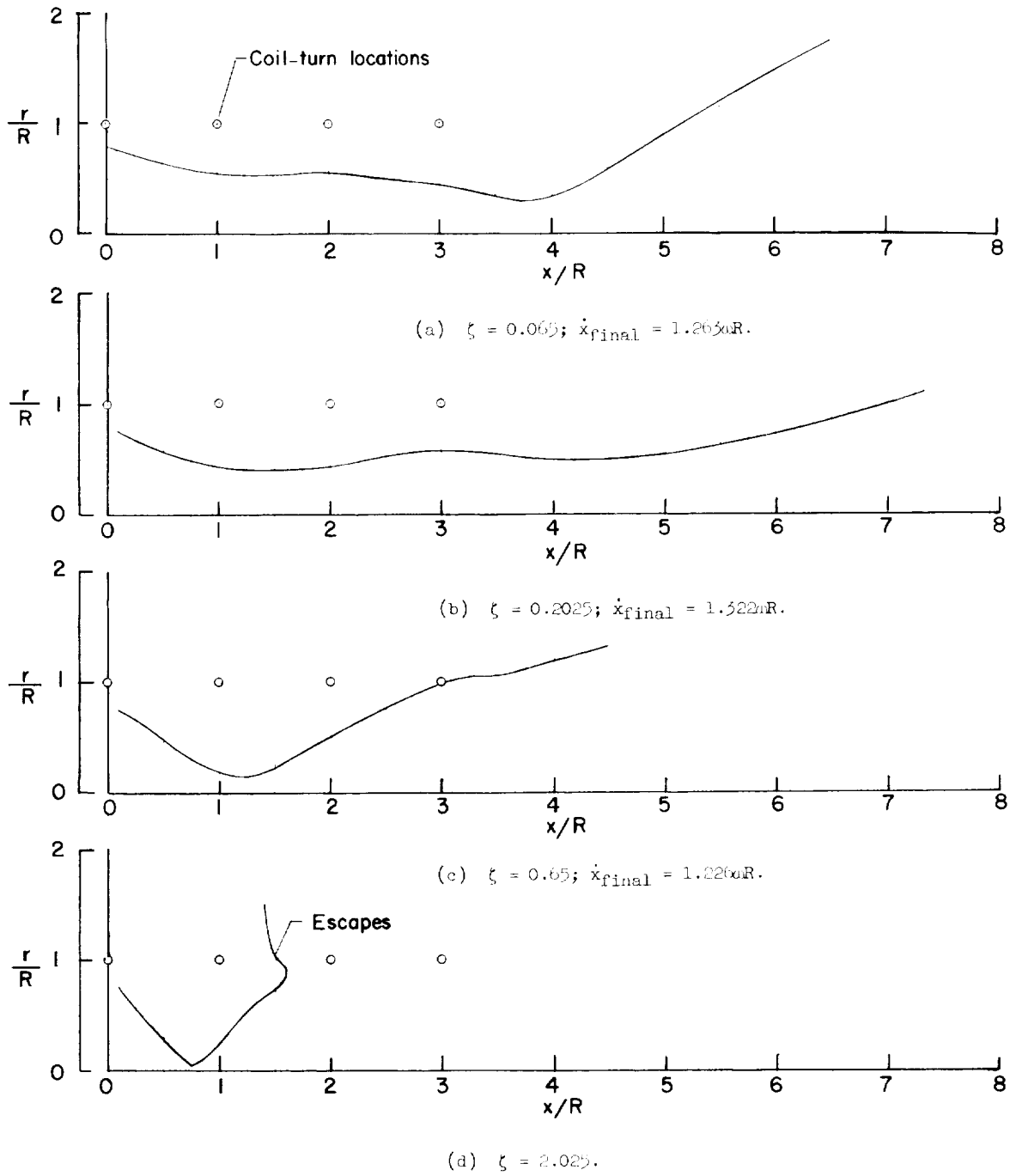

Figure 5.- Paths of an argon plasma ring in the field of accelerator IV, a 4-coil, four-phase traveling-magnetic-wave system. B = 150; β = 73,690; starting conditions: $\dot{x}_o = 0$, $\dot{r}_o = \theta_o = t_o = 0$, $x_o/R = 0.1$, $r_o/R = 0.75$.

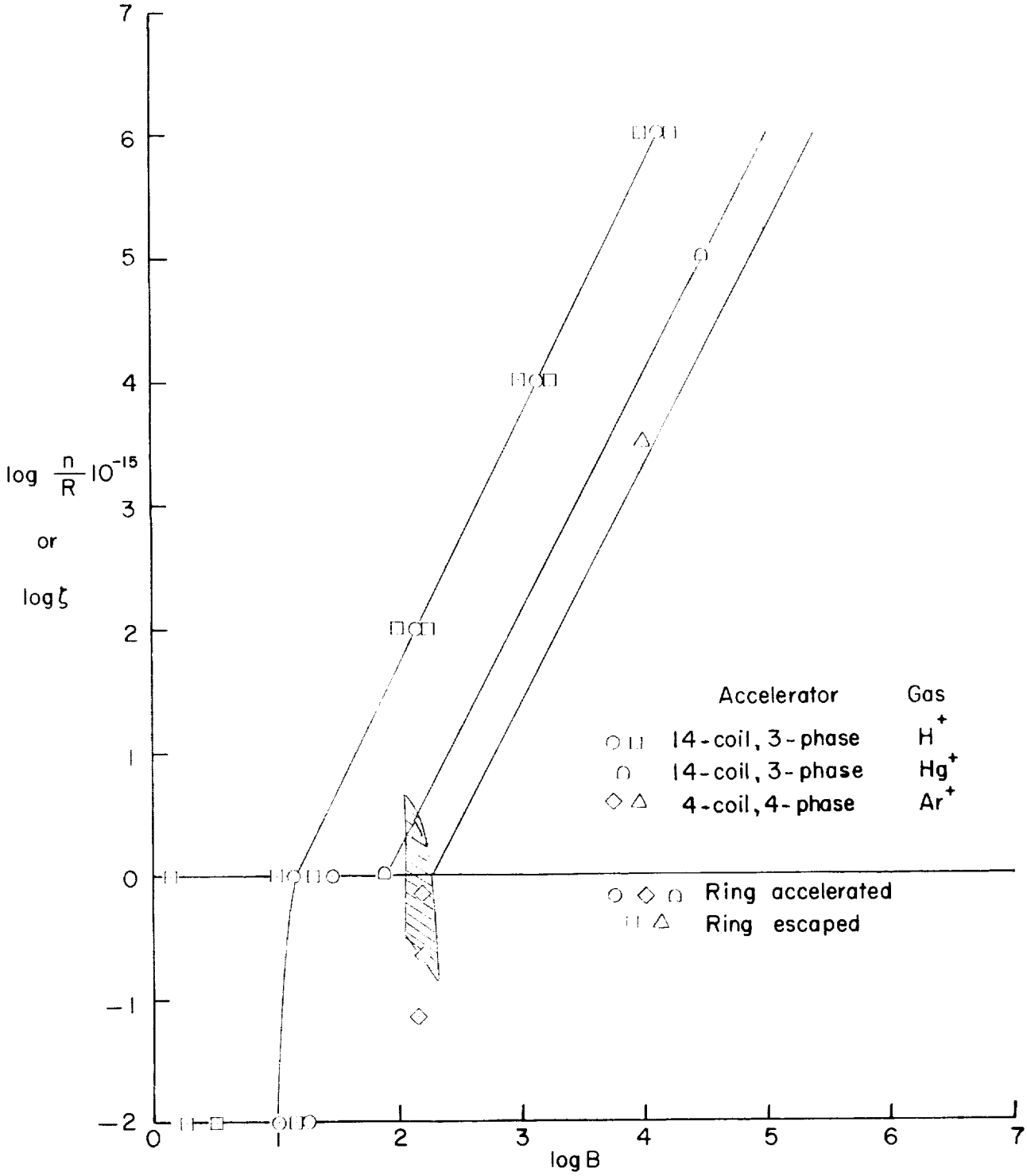

Figure 6.- Region of successful operation of accelerators I and IV shown as a function of log B and log ζ.

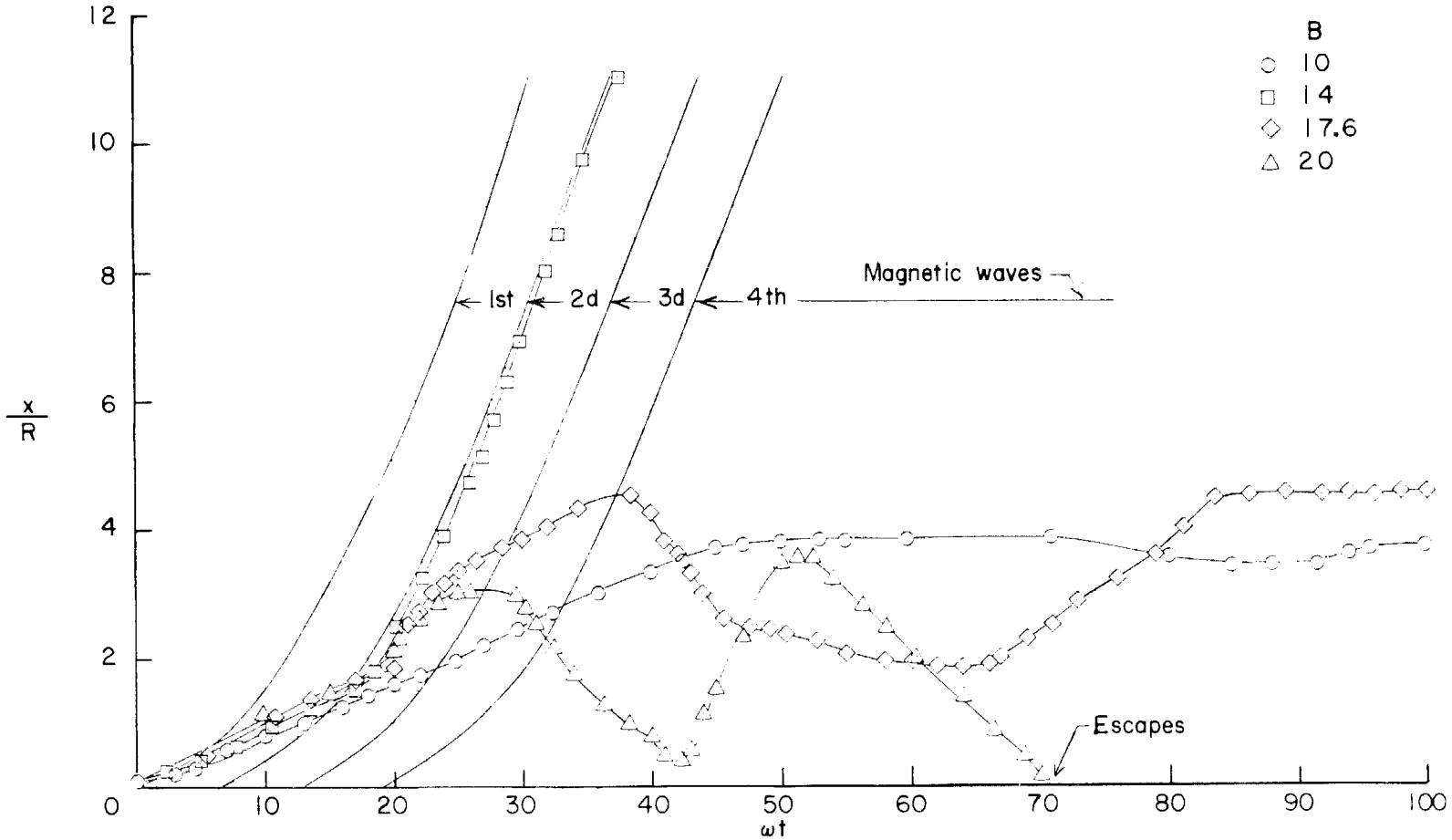

Figure 7.- Effects of changing B on the location of hydrogen plasma rings in accelerator I plotted as a function of nondimensional time. $r_0/R = 10^{-2}$ or $\zeta = 1$; $\beta = 1,8\frac{1}{2}$; $\dot{x}_0 = 0.0 \cdots 7\omega R$.

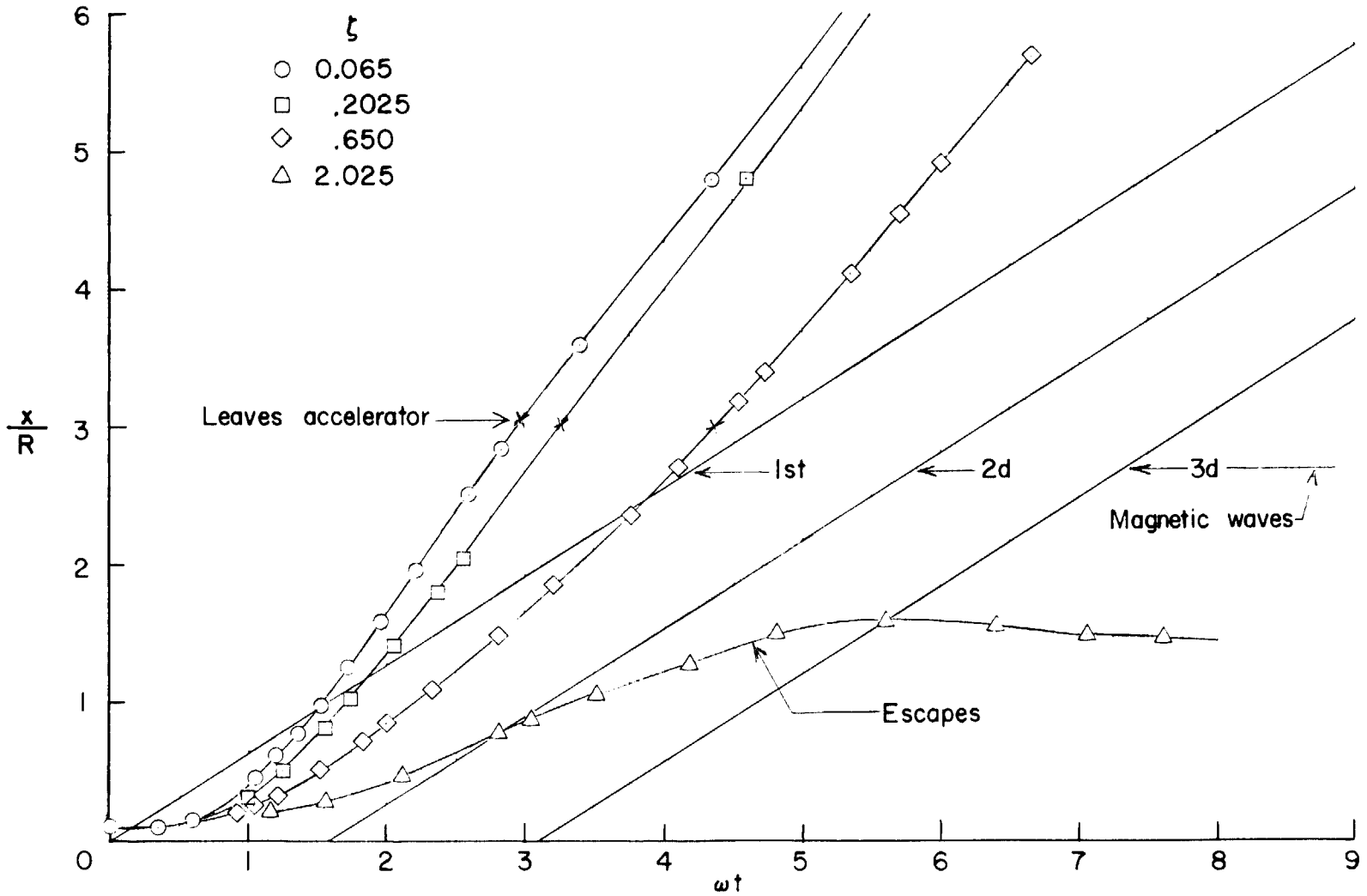

Figure 8.- Effects of changing ζ on the location of argon plasma rings in accelerator IV. B = 150; β = 73,690; $\dot{x}_o$ = 0.

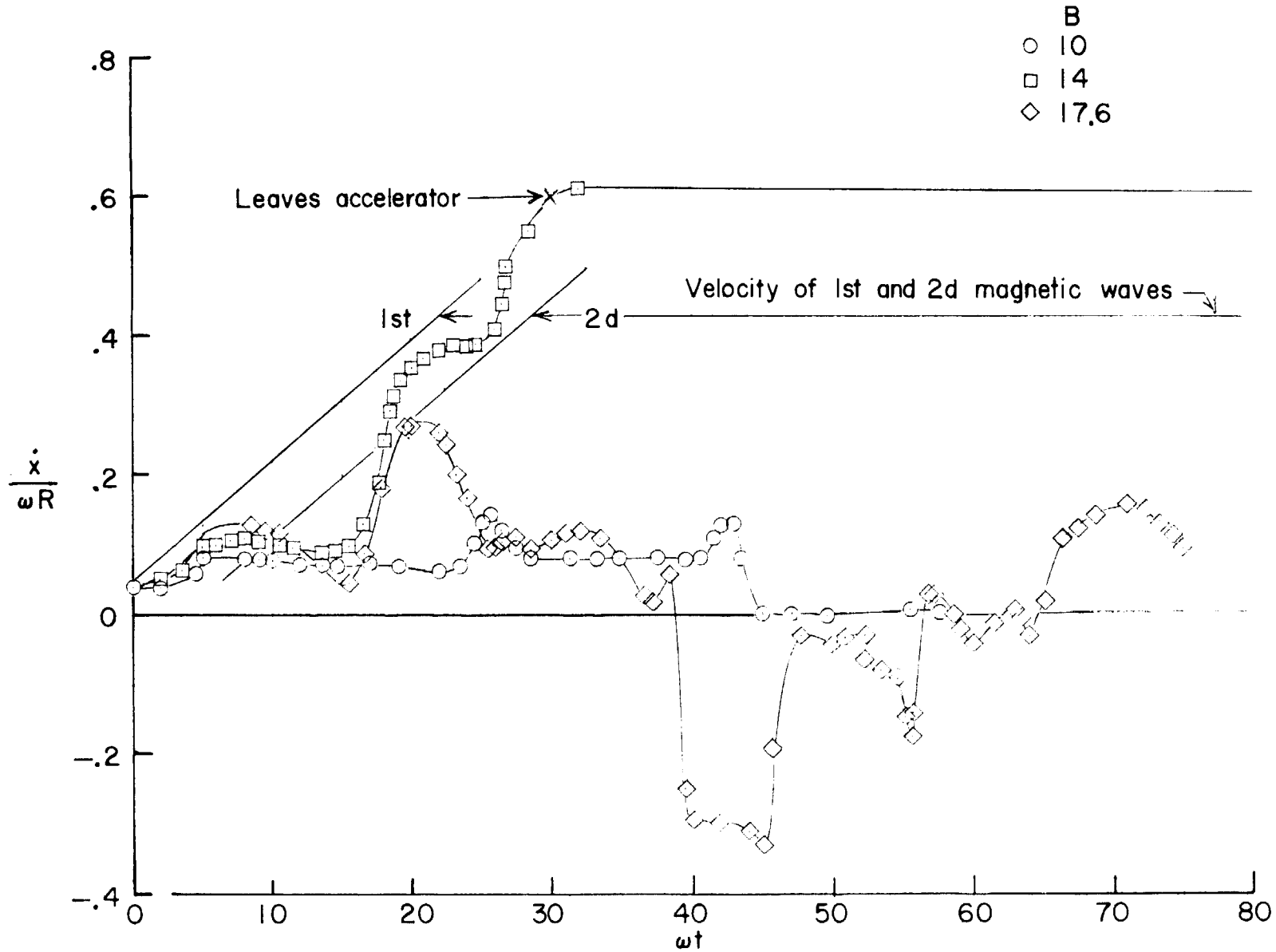

Figure 9.- Effects of changing B on the velocity of hydrogen plasma rings in accelerator 1. 1--coil, three-phase system; $n_i R = 10^{15}$; $\theta = 1,345$; $\dot{x}_0 = 0.0447\omega R$.

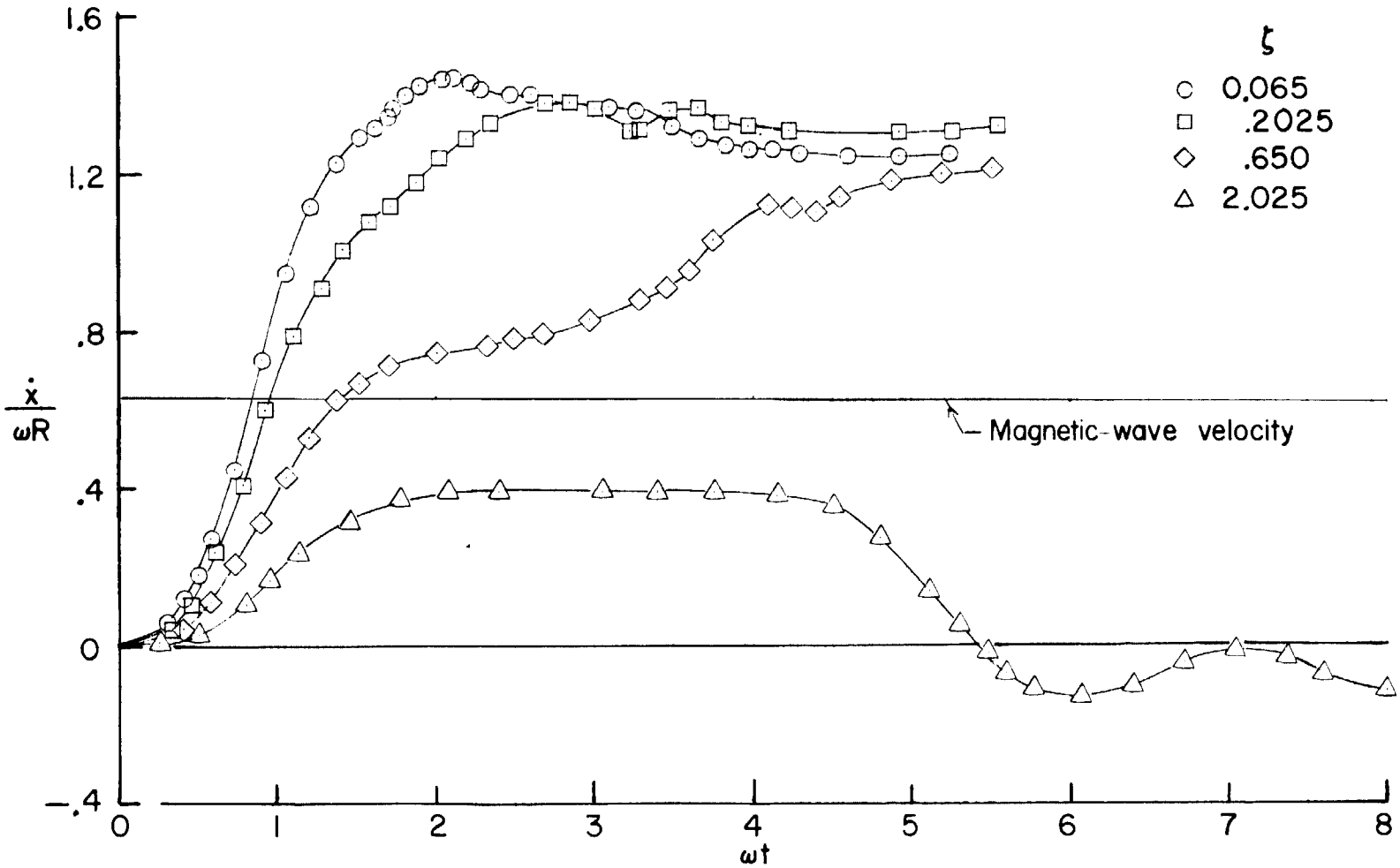

Figure 10.- Effects of changing ζ on the velocity of argon plasma rings in accelerator IV. $B = 150$; $\beta = 73{,}690$; $\dot{x}_o = 0$.

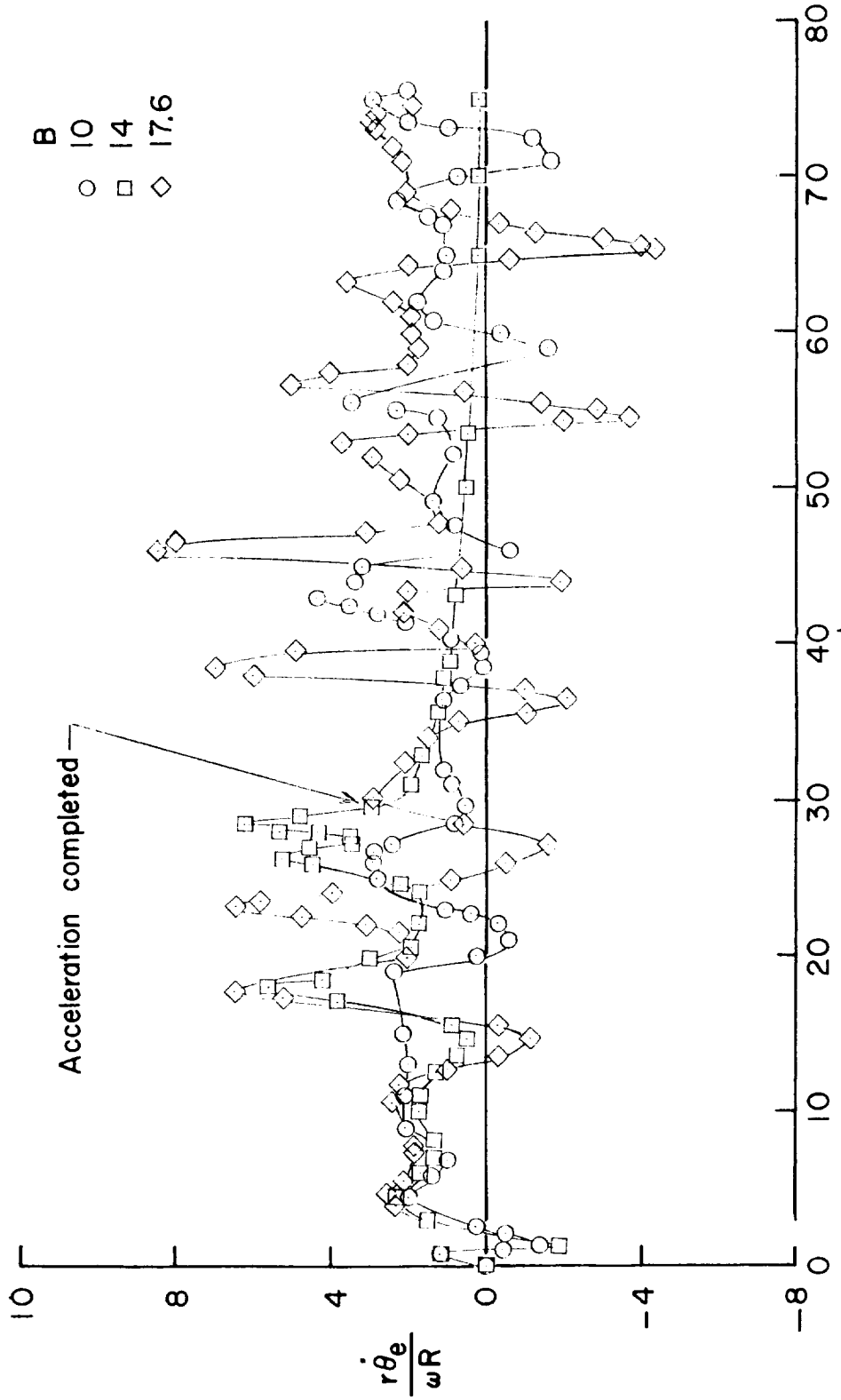

Figure 11.- Azimuthal electron velocity of several hydrogen rings in accelerator I. 14-coil, three-phase system; $n/R = 10^{15}$; $\beta = 1,845$.